Electronic supporting information

Intermittent Ultrasound-Assisted Anti-Solvent Crystallization for Sucralose Production with Ultra-low Aspect Ratio and Larger Crystal Size

Dongyu Zhou[a,b], Yongshang Li[a,b], Huimig Jie[a,b], Jiayan Lei[a,b], Zi'ang Chen[c], Xiaoping Chen[a,b], Can Cui[c], Huadong Luo[c], Jingjing Chen[a,b*], Haohong Li[a,d], Huidong Zheng[a,b*]

[a]*Engineering Research Center of Advanced Manufacturing Technology for Fine Chemicals (Fujian Province University), College of Chemical Engineering, Fuzhou University, Fuzhou, Fujian, 350108, P. R. China*

[b]*Qingyuan Innovation Laboratory, Quanzhou, Fujian, 362801, P. R. China*

[c]*Fujian Key Laboratory of Bio-based Food and Daily Chemical Additives, Techno Food Ingredients Co., Ltd, Sanming, Fujian, 366099, P. R. China*

[d]*College of Chemistry, Fuzhou University, Fuzhou, Fujian, 350108, P. R. China*

*E-mail addresses: jing_chem@fzu.edu.cn (J.-J. Chen), youngman@fzu.edu.cn (H. -D. Zheng)

Table S1 Crystal data and structural determinations of sucralose from four anti-solvents in ASC process

	IVA	HNA	ONA	DNA
Empirical formula	$C_{12}H_{19}Cl_3O_8$	$C_{12}H_{19}Cl_3O_8$	$C_{12}H_{19}Cl_3O_8$	$C_{12}H_{19}Cl_3O_8$
Formula mass	397.62	397.62	397.62	397.62
Crystal system	Orthorhombic	Orthorhombic	Orthorhombic	Orthorhombic
Space group	$P2_12_12_1$	$P2_12_12_1$	$P2_12_12_1$	$P2_12_12_1$
a[Å]	7.3167(6)	7.2691(14)	12.041 (4)	7.2843(6)
b[Å]	12.0459(10)	11.947(2)	7.3141(12)	12.0048(8)
c [Å]	18.1855(15)	17.987(3)	18.158(6)	18.0766(12)
V[Å^3]	1602.8(2)	1562.0(5)	1599.2(7)	1580.7(2)
Z	4	4	4	4
D_c[g/cm^3]	1.648	1.691	1.651	1.671
μ[mm^{-1}]	0.610	0.626	0.611	0.618
F(000)	824	824	824	824
Reflections collected	12477	8712	9234	9331
Reflections, unique	3738	3530	2750	3488
Reflections, observed	2883	2919	1553	3183
No. of parameters refined	213	213	213	213
$R_1[I>2\sigma(I)]$	0.0671	0.040	0.0572	0.0303
wR_2 $[I>2\sigma(I)]$	0.1591	0.1040	0.1279	0.0876
Residual extremes (e/Å^3)	0.570,-0.602	0.407,-0.468	0.323, -0.327	0.392, -0.354

Table S2 Selected bond lengths of sucralose products from four anti-solvents in ASC process (in Å)

	Bond length	IVA	HNA	ONA	DNA
	C(2)-C(3)	1.524(8)	1.506(6)	1.503(13)	1.517(4)
	C(3)-C(4)	1.527(8)	1.526(6)	1.518(13)	1.536(4)
	C(4)-C(5)	1.515(8)	1.516(5)	1.504(13)	1.522(4)
	C(5)-C(6)	1.536(7)	1.516(6)	1.534(13)	1.524(4)
	C(2)-O(2)	1.442(6)	1.435(5)	1.444(11)	1.435(3)
glucopyranosyl ring	C(6)-O(2)	1.415(6)	1.413(5)	1.408(11)	1.411(3)
	C(1)-C(2)	1.505(8)	1.505(6)	1.495(13)	1.508(4)
	C(4)-O(3)	1.410(6)	1.409(5)	1.421(10)	1.406(3)
	C(5)-O(4)	1.418(6)	1.416(5)	1.414(11)	1.417(4)
	C(1)-O(1)	1.436(7)	1.425(5)	1.426(11)	1.437(4)
	C(3)-Cl(1)	1.802(5)	1.798(4)	1.796(10)	1.804(3)
	C(8)-C(9)	1.558(7)	1.541(5)	1.550(14)	1.558(4)
	C(9)-C(10)	1.524(8)	1.513(6)	1.517(13)	1.522(4)
	C(10)-C(11)	1.526(8)	1.518(5)	1.516(13)	1.526(4)
	C(8)-O(6)	1.419(6)	1.421(5)	1.432(12)	1.426(3)
fructofuranosyl ring	C(11)-O(6)	1.457(6)	1.439(5)	1.448(11)	1.446(3)
	C(7)-C(8)	1.533(7)	1.527(6)	1.540(12)	1.533(4)
	C(7)-Cl(2)	1.785(5)	1.787(4)	1.783(9)	1.790(3)
	C(11)-C(12)	1.498(8)	1.506(6)	1.484(14)	1.505(4)

	C(12)-Cl(3)	1.793(6)	1.778(4)	1.782(11)	1.788(3)
	C(10)-O(7)	1.417(6)	1.404(5)	1.414(10)	1.412(3)
	C(9)-O(8)	1.420(7)	1.417(5)	1.411(11)	1.415(4)
linkage	C(6)-O(5)	1.426(6)	1.432(4)	1.427(11)	1.434(3)
	C(8)-O(5)	1.424(6)	1.412(5)	1.411(10)	1.415(3)
	C(6)-O(5)-C(8)	119.307°	118.968	119.243	119.356°

Table S3. Hydrogen bonding details of sucralose using IVA as anti-solvent

	D-H···A	D–H/Å	H···A/Å	D···A/Å	∠(D–H···A)/°	Symmetry codes
Intra-molecular	O(4)-H(9)···O(8)	0.82	1.99	2.797(6)	168.6	
Inter-molecular	O(3)-H(6)···O(1)	0.82	1.94	2.761(6)	176.6	1+x,y,z
	O(8)-H(14)···O(3)	0.82	1.92	2.733(5)	174.9	2-x,-1/2+y,1/2-z
	O(7)-H(16)···O(4)	0.82	1.94	2.748(5)	168.9	2-x,-1/2+y,1/2-z

Table S4. Hydrogen bonding details of sucralose using HNA as anti-solvent

	D-H···A	D–H/Å	H···A/Å	D···A/Å	∠(D–H···A)/°	Symmetry codes
Intra-molecular	O(4)-H(9)···O(8)	0.82	1.96	2.770(4)	169.7	
Inter-molecular	O(3)-H(6)···O(1)	0.82	1.91	2.723(4)	168.6	1+x,y,z
	O(8)-H(14)···O(3)	0.82	1.89	2.710(4)	174.5	2-x,1/2+y,3/2-z
	O(7)-H(16)···O(4)	0.82	1.90	2.723(4)	175.8	2-x,1/2+y,3/2-z
	C(1)-H(3)···Cl(2)	0.97	2.79	3.733(4)	164.1	1/2+x,1/2-y,1-z

Table S5. Hydrogen bonding details of sucralose using ONA as anti-solvent

	D-H···A	D–H/Å	H···A/Å	D···A/Å	∠(D–H···A)/°	Symmetry codes
Intra-molecular	O(4)-H(9)···O(8)	0.82	2.00	2.799(10)	165.7	
Inter-molecular	O(3)-H(6)···O(1)	0.82	1.95	2.769(10)	176.2	x,-1+y,z
	O(8)-H(14)···O(3)	0.82	1.92	2.737(9)	172.4	-1/2+x,1/2-y,1-z
	O(7)-H(16)···O(4)	0.82	1.94	2.755(9)	173.2	-1/2+x,1/2-y,1-z
	C(1)-H(3)···Cl(2)	0.97	2.81	3.754(11)	165.2	1-x,-1/2+y,3/2-z

Table S6. Hydrogen bonding details of sucralose using DNA as anti-solvent

	D-H···A	D–H/Å	H···A/Å	D···A/Å	∠(D–H···A)/°	Symmetry codes
Intra-molecular	O(4)-H(9)···O(8)	0.82	1.97	2.784(3)	169.8	
Inter-molecular	O(3)-H(6)···O(1)	0.82	1.92	2.735(3)	176.9	1+x,y,z
	O(8)-H(14)···O(3)	0.82	1.91	2.723(3)	174.3	2-x,1/2+y,3/2-z
	O(7)-H(16)···O(4)	0.82	1.91	2.732(3)	175.8	2-x,1/2+y,3/2-z
	C(1)-H(3)···Cl(2)	0.97	2.80	3.748(3)	165.2	1/2+x,1/2-y,1-z

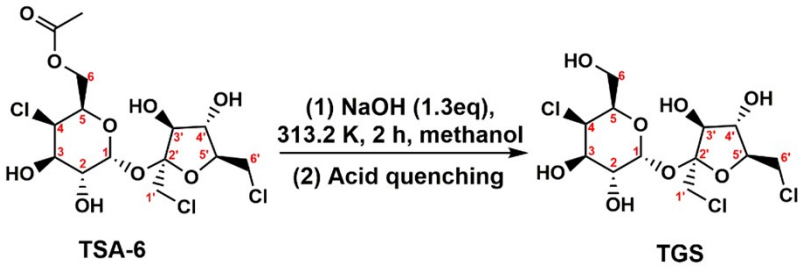

Scheme 1 Alcoholysis of 4,1',6'-trichlorosucrose-6-acetate (TSA-6) to TGS

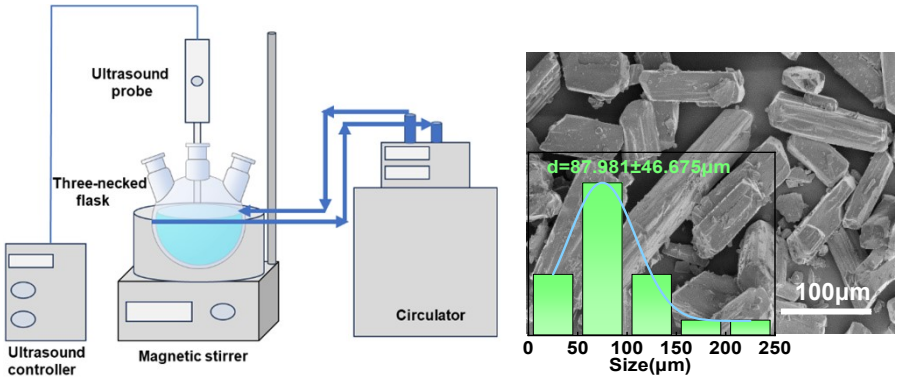

(a) (b)

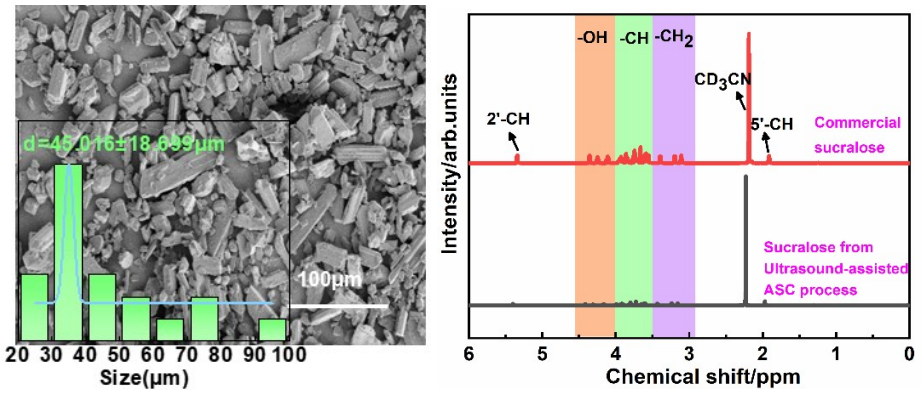

(c) (d)

Fig. S1 (a) Schematic diagram of ultrasound-assisted ASC; (b) SEM of the commercial sucralose; (c) SEM of sucralose obtained from ethanol without addition of anti-solvent; (d) ^{1}H NMR spectra of sucralose from ultrasound-assisted ASC and commercial source

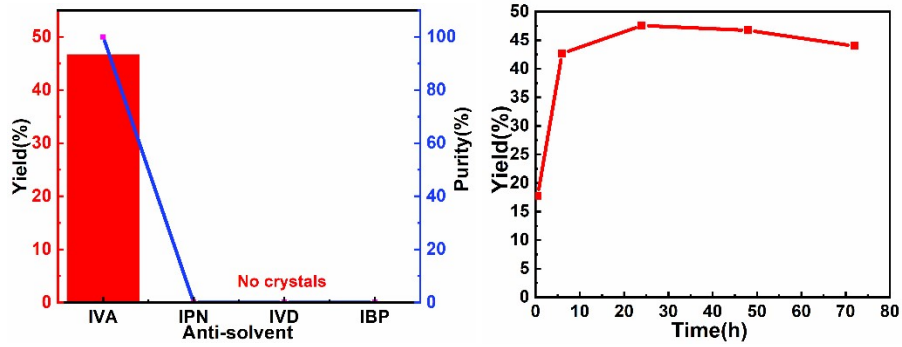

(a) (b)

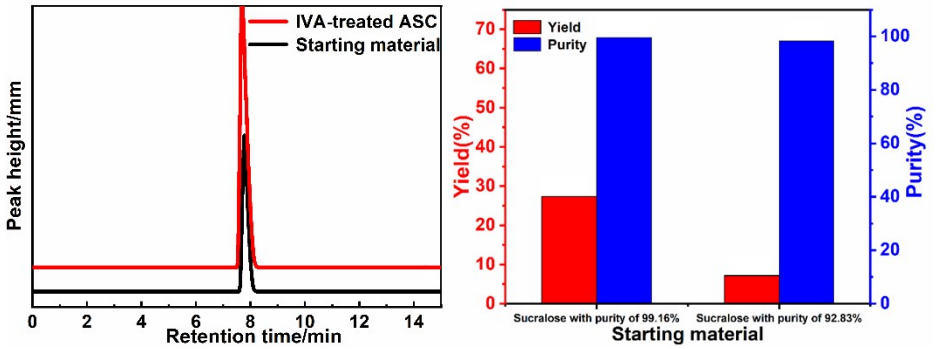

(c) (d)

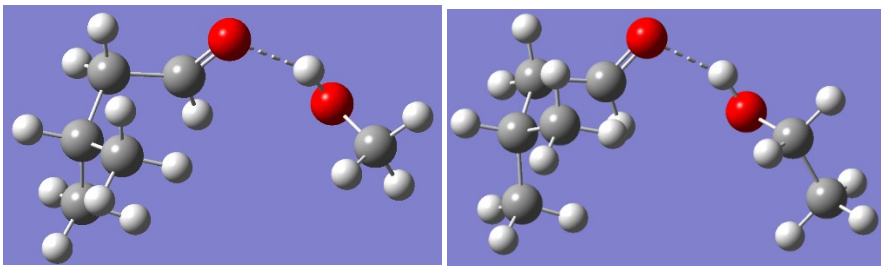

(e) (f)

Fig. S2 (a) Ethanol-based ASC yield/purity of sucralose at 48 h; (b) crystallizing yield using IVA as anti-solvent at different time; (c) HPLC diagrams in ASC process using IVA as anti-solvent at 48 h; (d) yield/purity in traditional water-involved process; the optimized geometries: (e) methanol··· IVA; (f) ethanol··· IVA

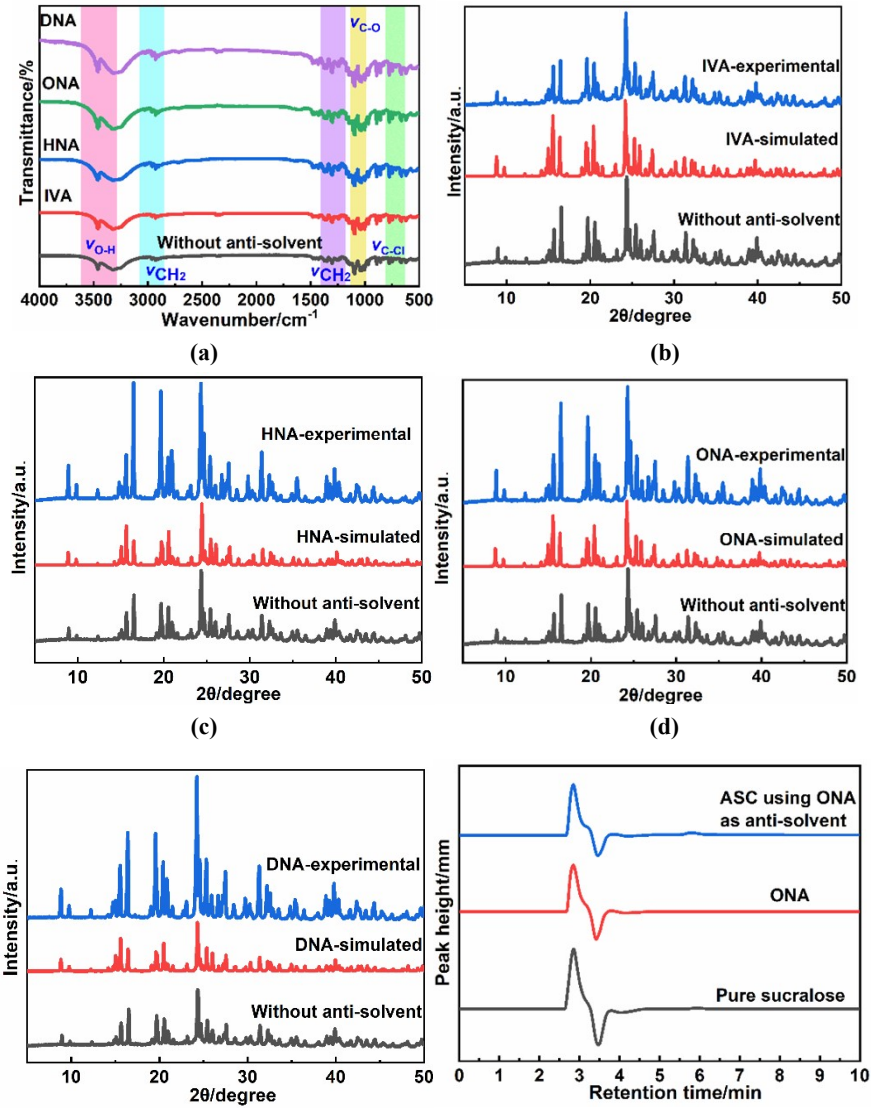

(a) (b)

(c) (d)

(e) (f)

Fig. S3 Characterizations of four sucrolose products obtained from ASC with different anti-solvents: (a) FT-IR spectra; experimental and simulated PXRD: (b) IVA; (c) HNA; (d) ONA; (e) DNA; (f) HPLC diagrams of sucralose, ONA and ASC system using ONA as anti-solvent

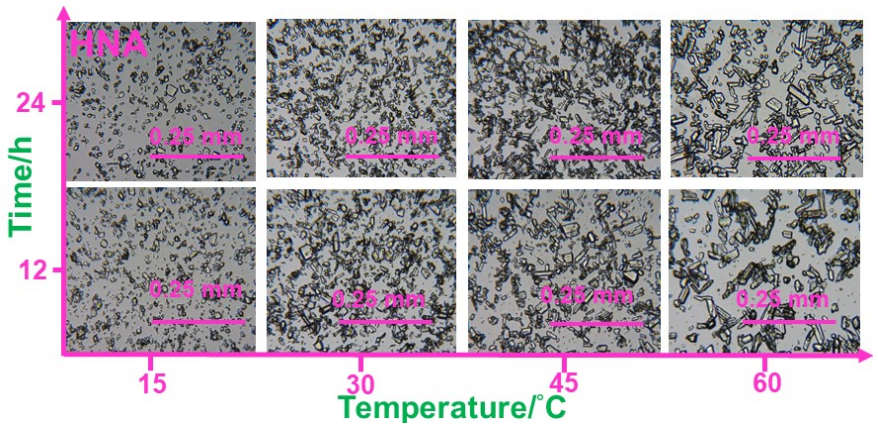

(a)

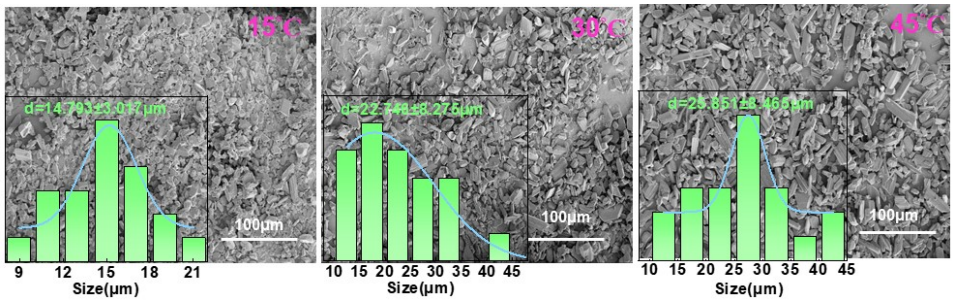

(b)

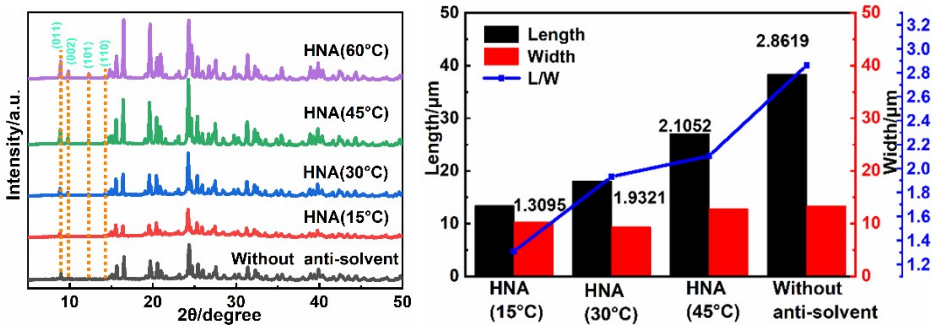

(c) (d)

Fig. S4 Effect of temperature on ASC using HNA as anti-solvent: (a) the light microscope diagrams; (b) SEM images showing the particle size distributions; (c) PXRD patterns; (d) length/width and aspect ratio

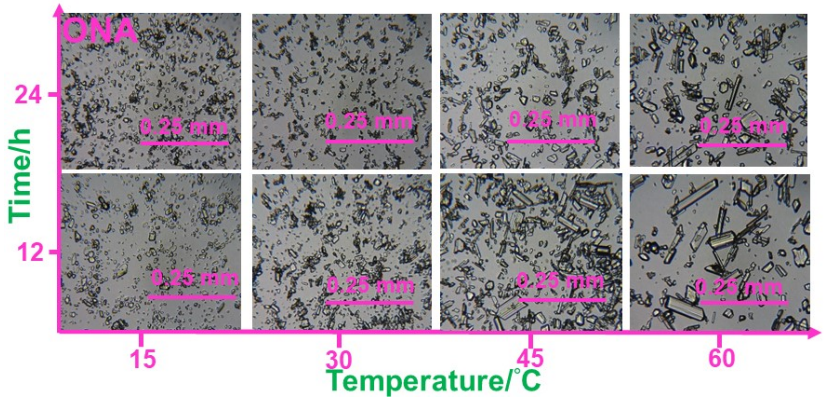

Fig. S5 Light microscope diagrams during ASC using ONA as anti-solvents under different temperature

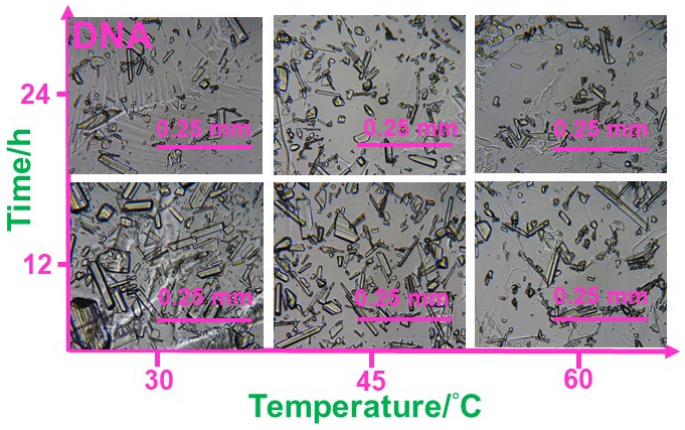

(a)

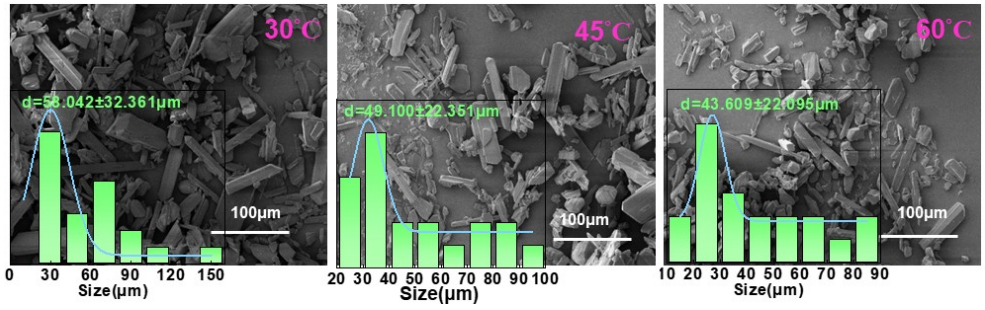

(b)

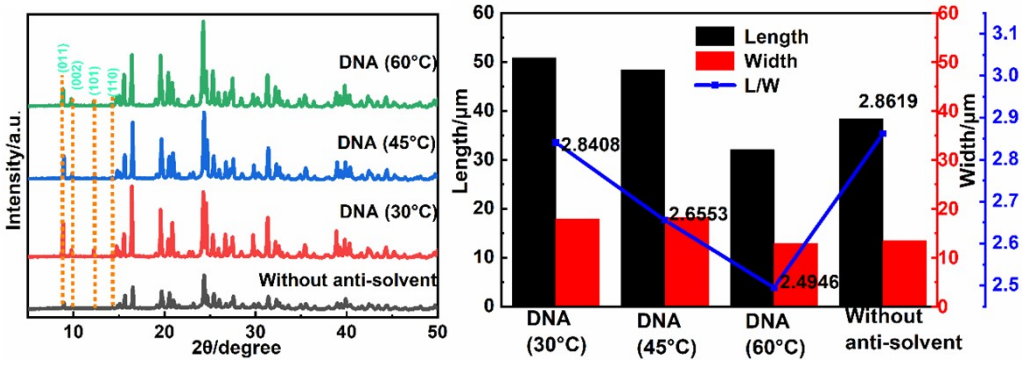

(c) (d)

Fig. S6 The effect of temperature on ASC using DNA as anti-solvent: (a) the light microscope diagrams; (b) SEM images showing the particle size distributions; (c) PXRD patterns; (d) length/width and aspect ratio

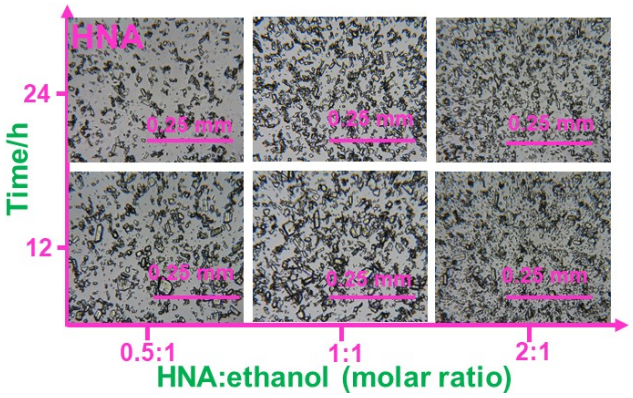

(a)

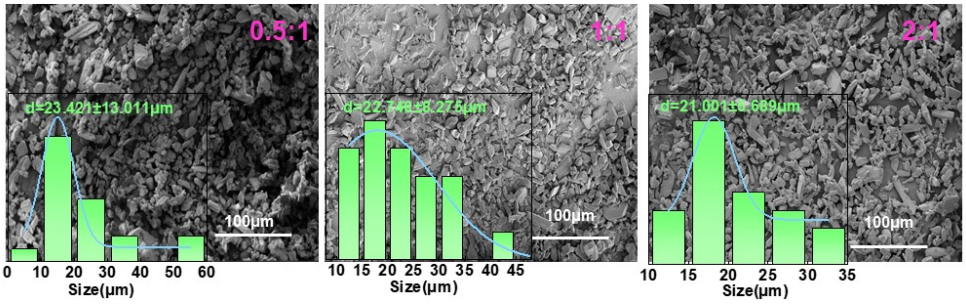

(b)

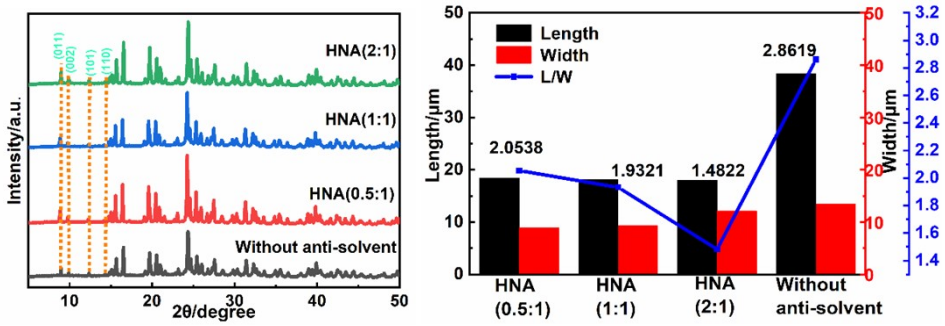

(c) (d)

Fig. S7 The effect of anti-solvent: ethanol molar ratio on ASC using HNA as anti-solvent: (a) the light microscope diagrams; (b) SEM images showing the particle size distributions; (c) PXRD patterns; (d) length/width and aspect ratio

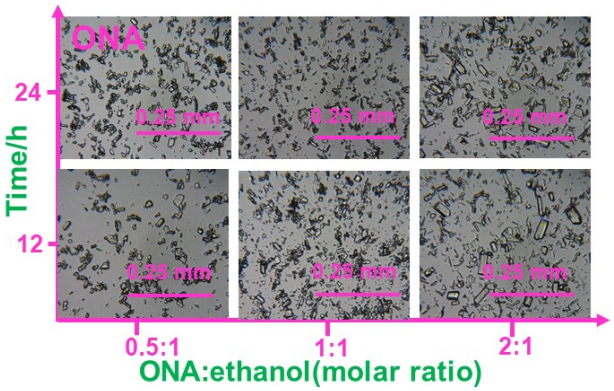

Fig. S8 Light microscope diagrams during ASC using ONA as anti-solvents under different ONA: ethanol molar ratio

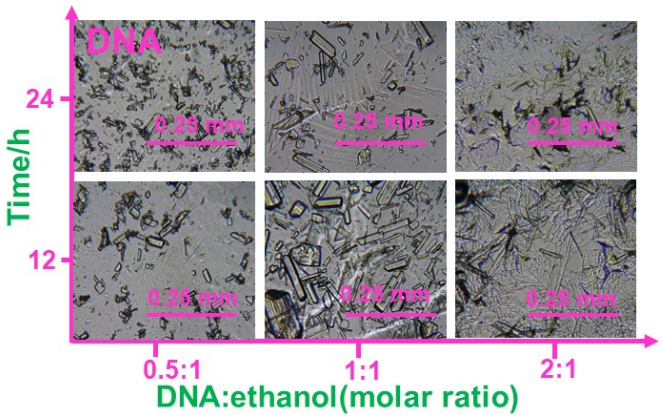

(a)

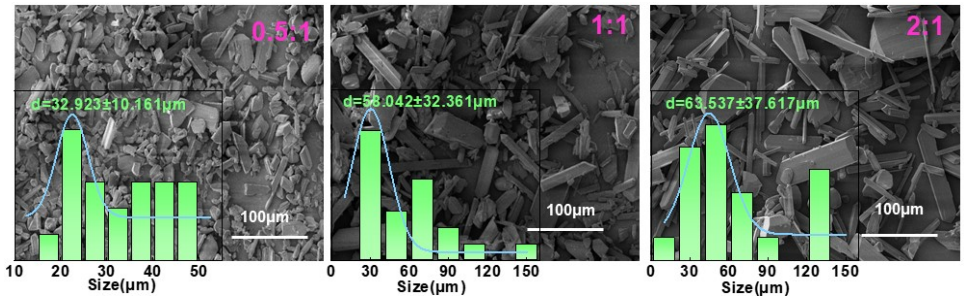

(b)

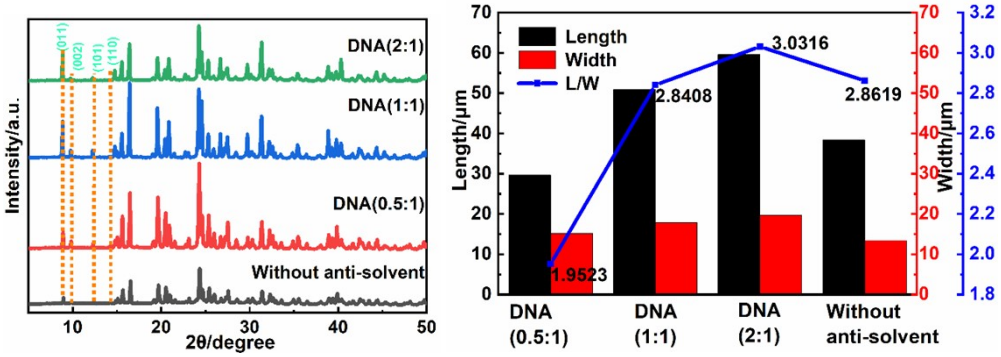

(c) (d)

Fig. S9 The effect of anti-solvent: ethanol molar ratio on ASC using DNA as anti-solvent: (a) the light microscope diagrams; (b) SEM images showing the particle size distributions; (c) PXRD patterns; (d) length/width and aspect ratio

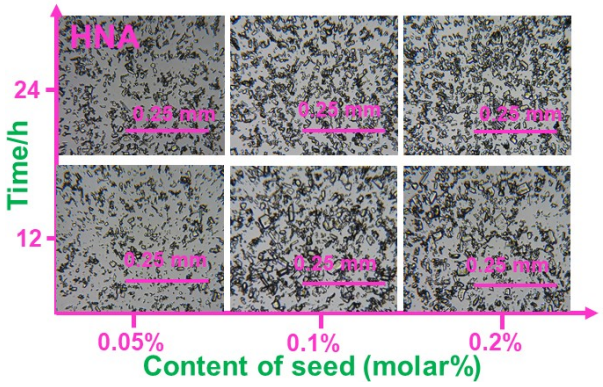

(a)

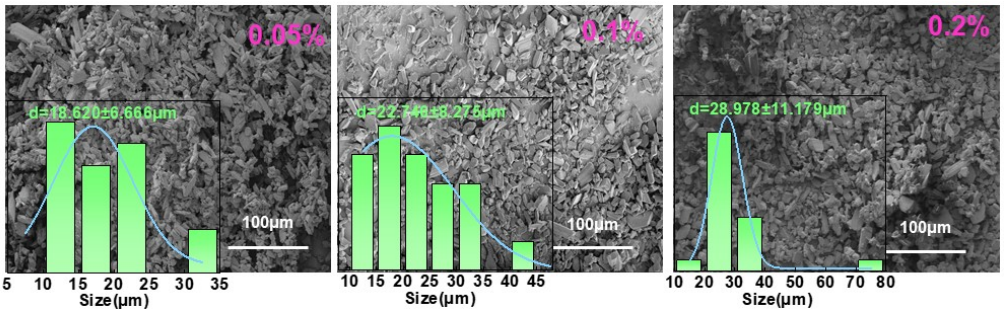

(b)

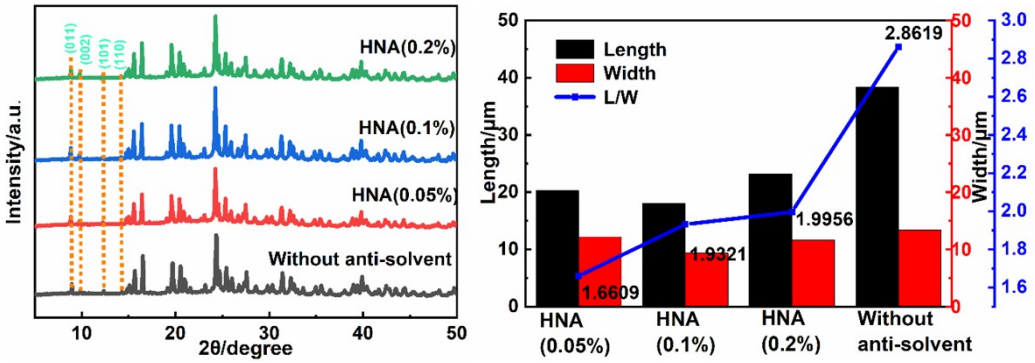

(c) (d)

Fig. S10 The effect of seed crystal content on ASC using HNA as anti-solvent: (a) the light microscope diagrams; (b) SEM images showing the particle size distributions; (c) PXRD patterns; (d) length/width and aspect ratio

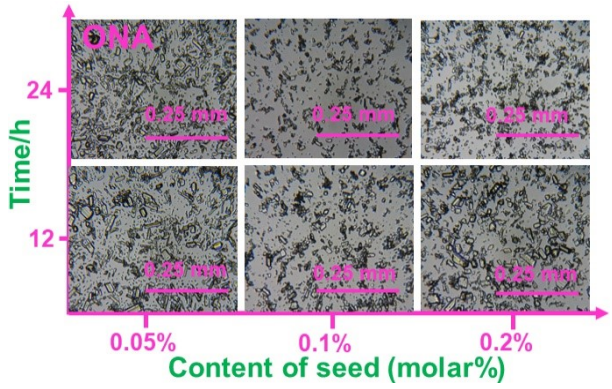

(a) (b)

Fig. S11 Light microscope diagrams during ASC using ONA as anti-solvents under different seed crystal content

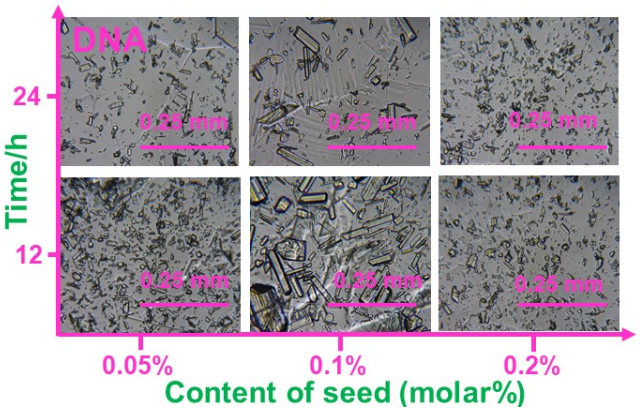

(a)

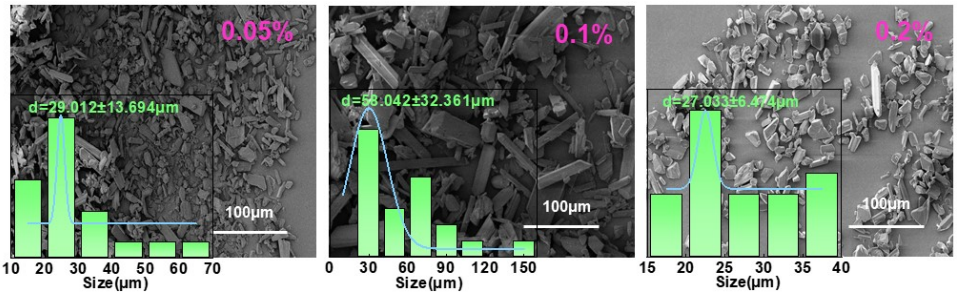

(b)

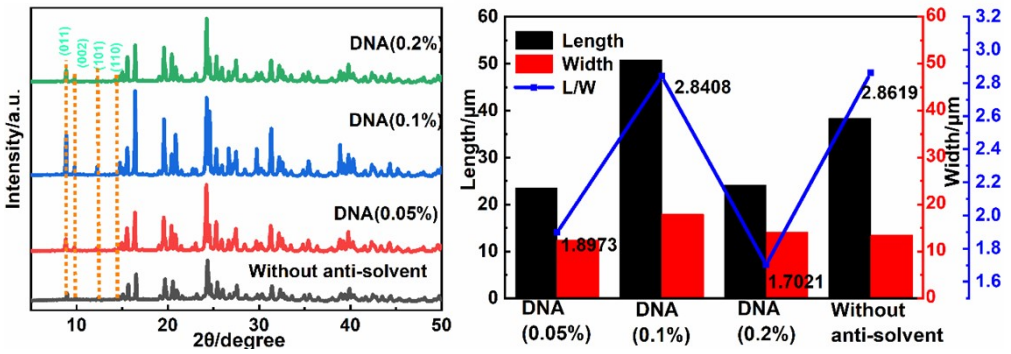

(c) (d)

Fig. S12 The effect of seed crystal content on ASC using DNA as anti-solvent: (a) the light microscope diagrams; (b) SEM images showing the particle size distributions; (c) PXRD patterns; (d) tlength/width and aspect ratio

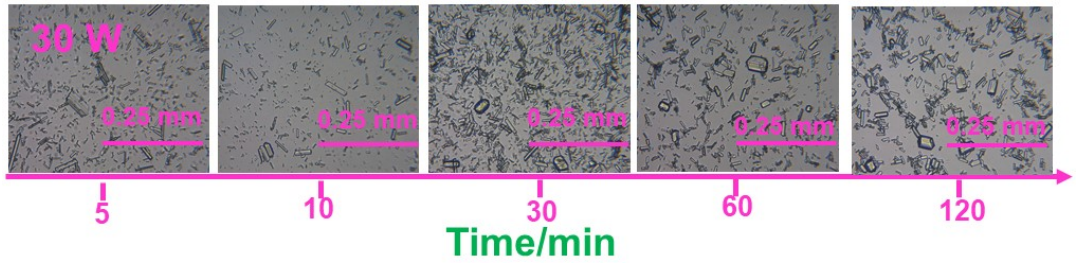

(a)

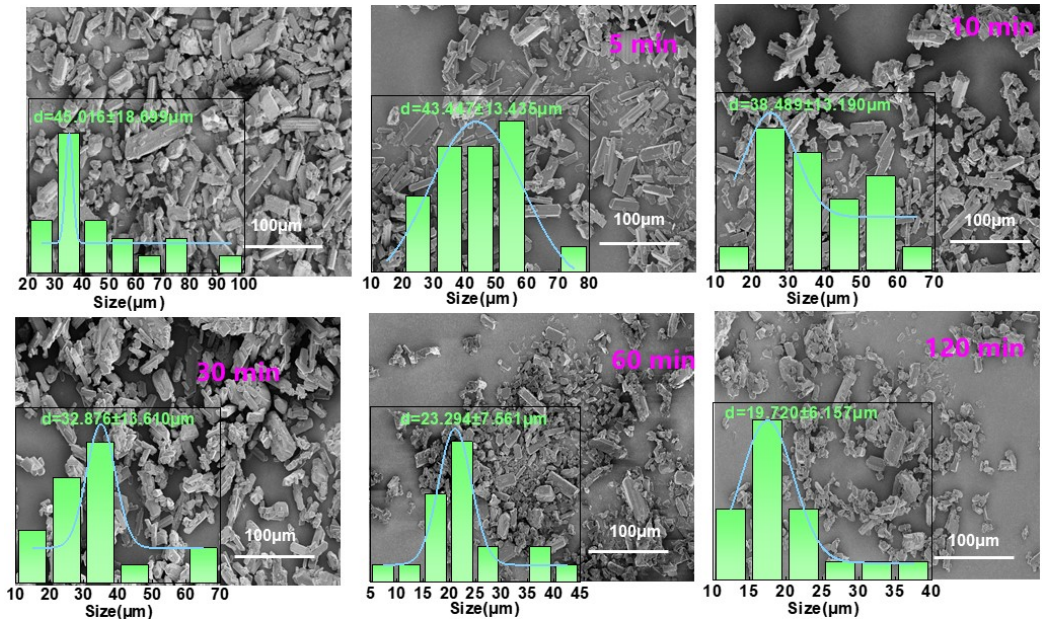

(b)

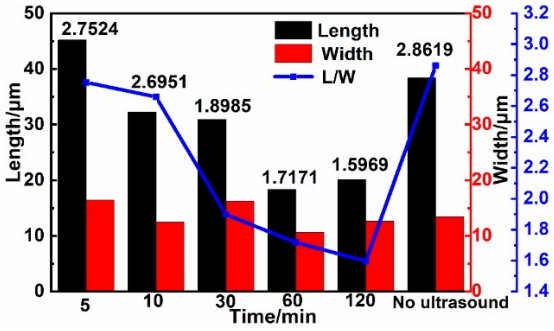

(c)

Fig. S13 (a) the light microscope diagrams of ultrasound-assisted ASC process at different sonication time; (b) SEM images showing the particle size distributions at different sonication times without ASC; (c) length/width and aspect ratio at different sonication times without ASC

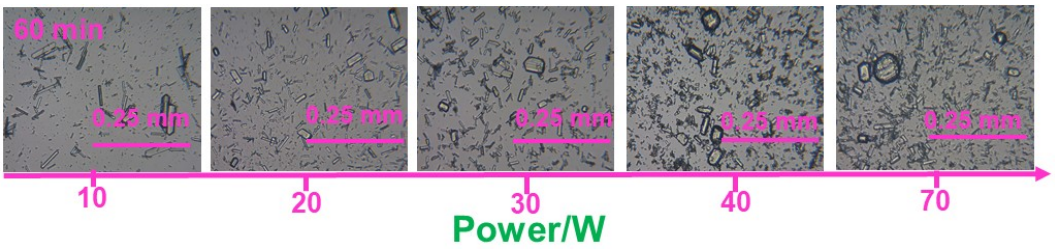

(a)

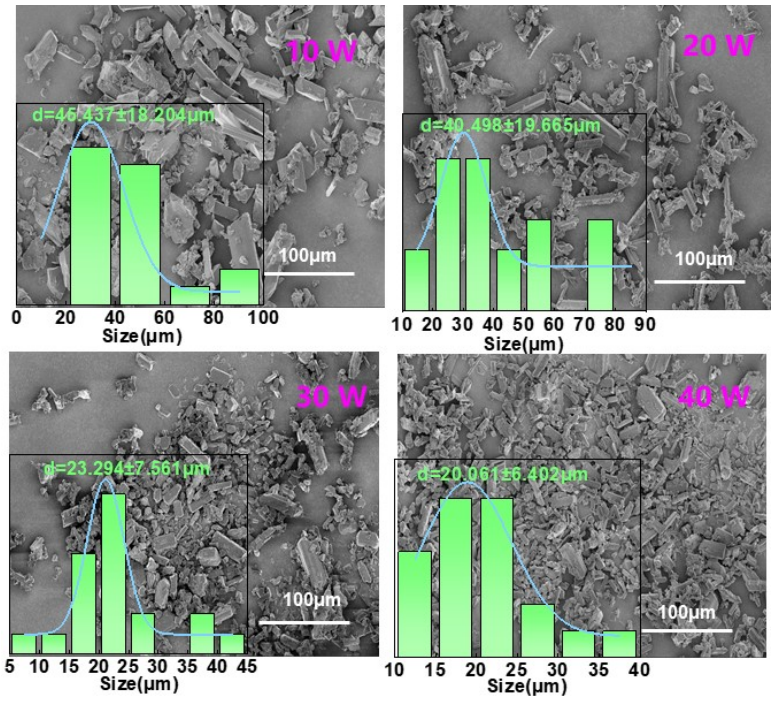

(b)

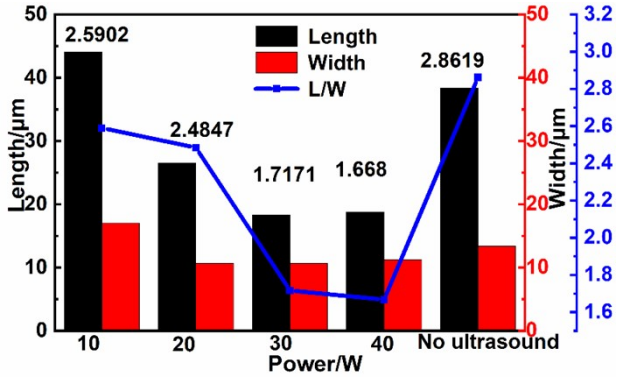

(c)

Fig. S14 (a) the light microscope diagrams of ultrasound-assisted ASC process under different sonication power; (b) SEM images showing the particle size distributions at different sonication power without ASC; (c) length/width and aspect ratio at different sonication power without ASC

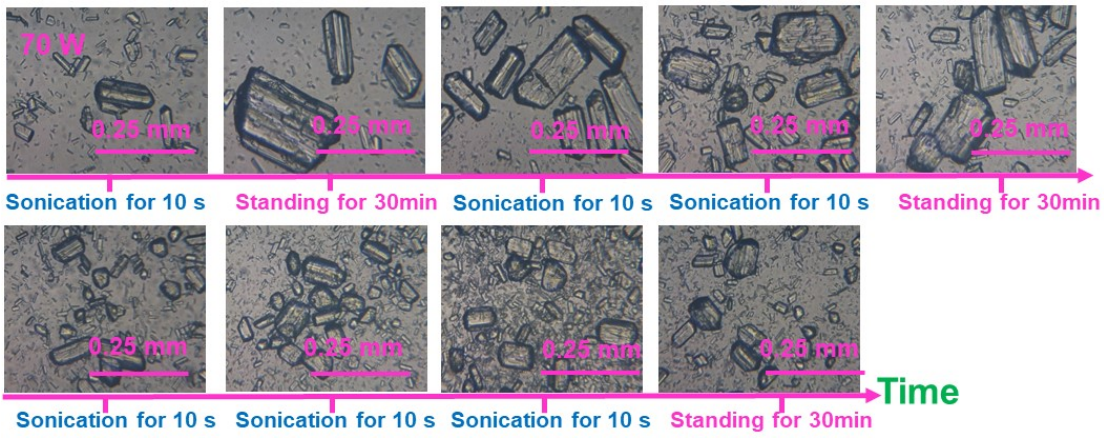

(a)

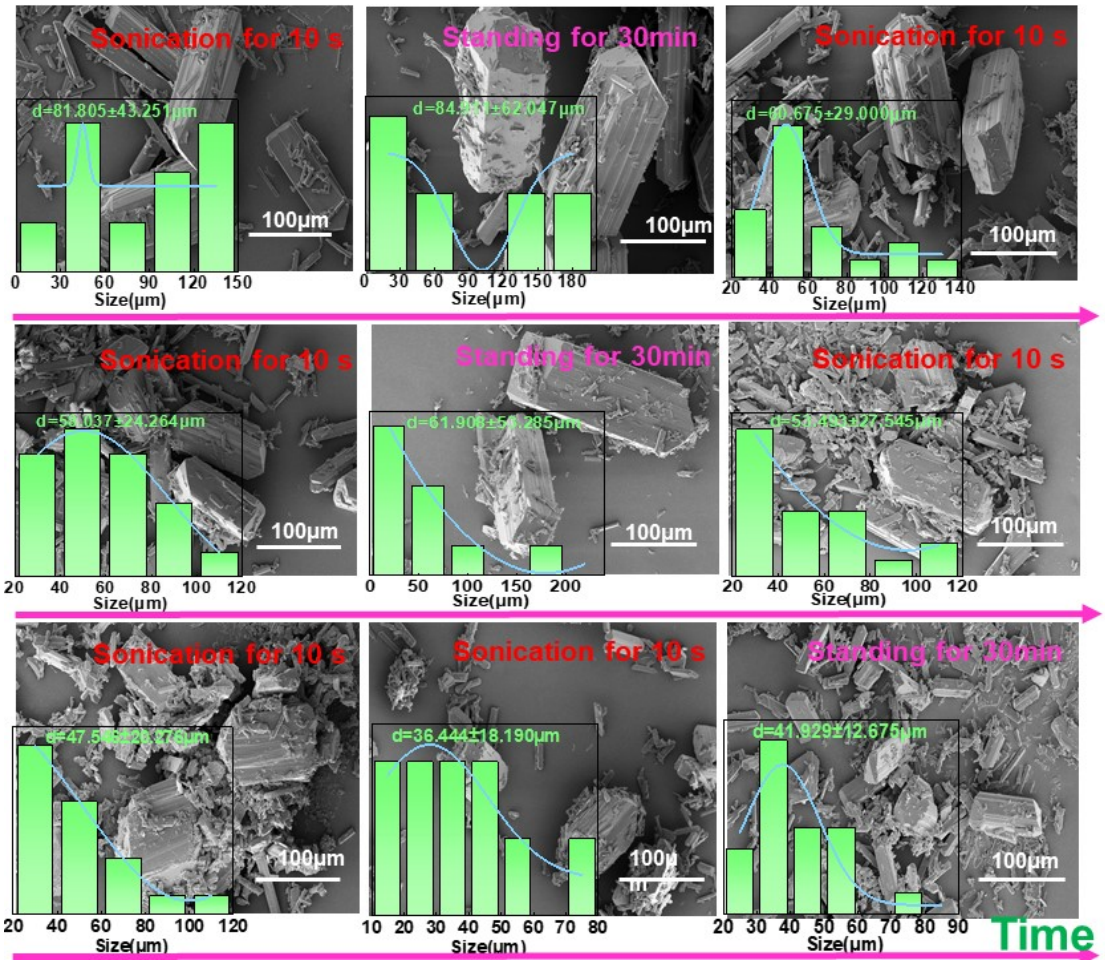

(b)

Fig. S15 (a) the light microscope diagrams of ASC process assisted by intermittent sonication: (a) discontinuous sonication time of 10, 20 and 30 s with 30 min standing time; (b) SEM images showing the particle size distributions

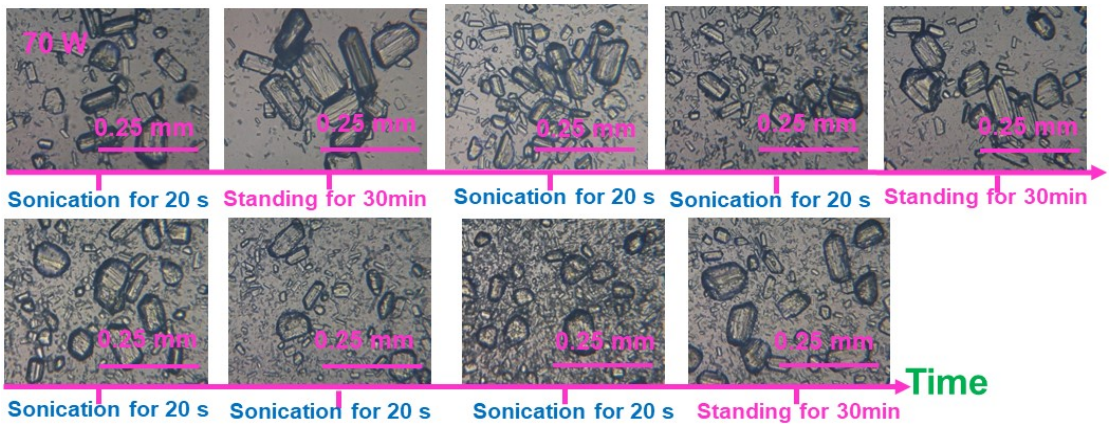

(a)

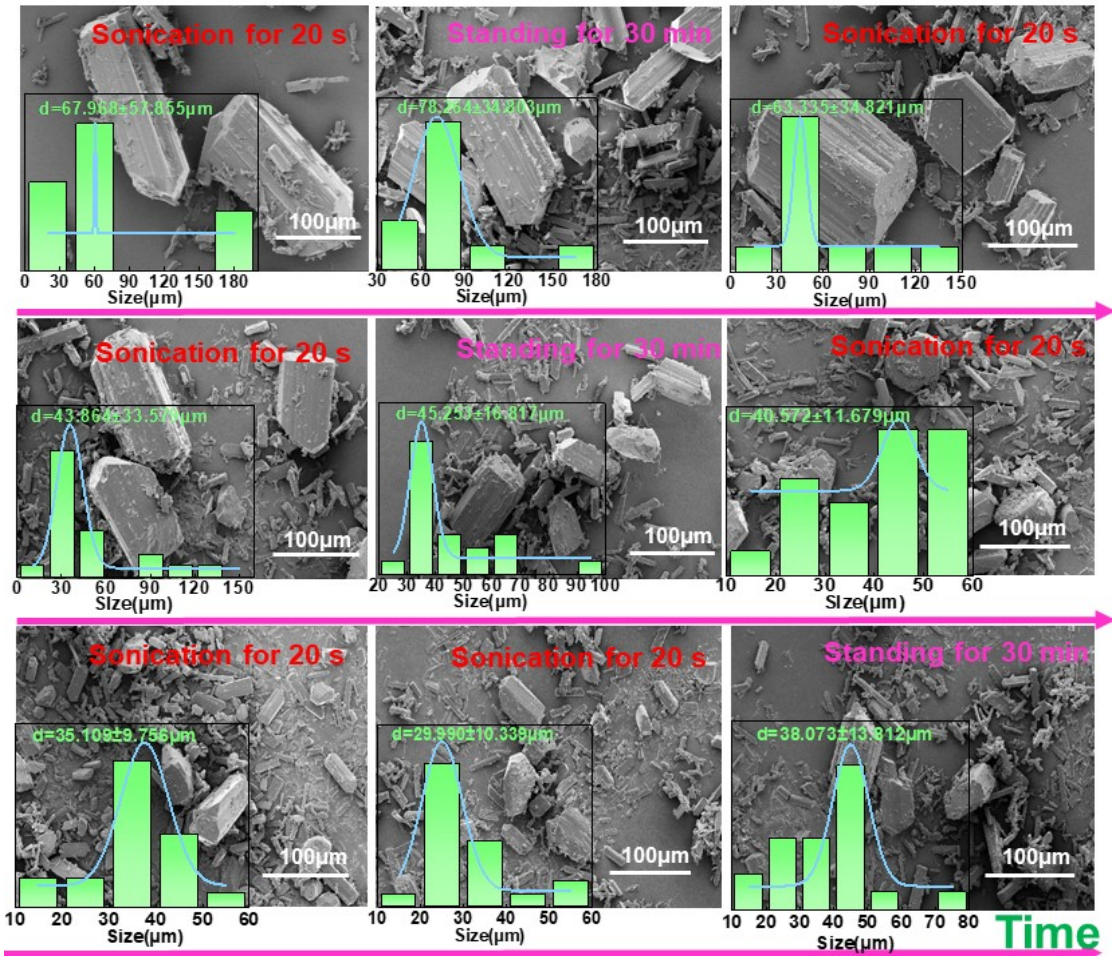

(b)

Fig. S16 (a) the light microscope diagrams of ASC process assisted by intermittent sonication: (a) discontinuous sonication time of 20, 40 and 60 s with 30 min standing time; (b) SEM images showing the particle size distributions

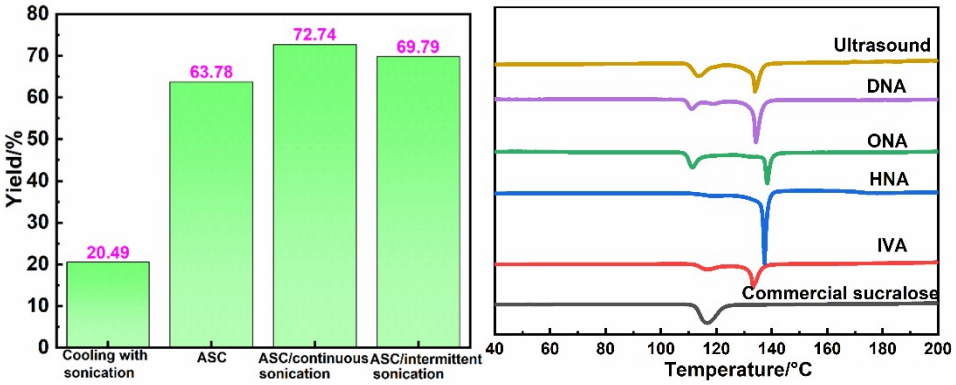

(a) (b)

Fig. S17 (a) Crystallization yields under different processes; (b) DSC curves of sucralose under different conditions

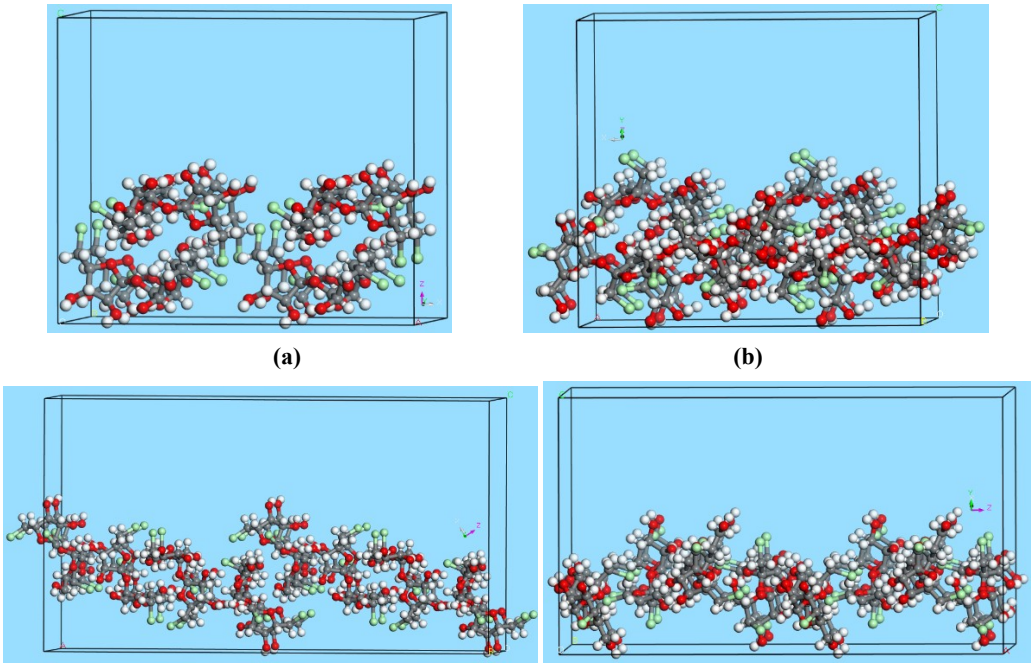

(a) (b)

Fig. S18 Four crystal faces of sucralose obtained from ethanol/ONA ASC: (a) {002} face; (b) {011} face; (c) {101} face; (d) {110} face